Pentamethylcyclopentadienylrhodaborane Chemistry. Part 4.[1] The Isolation, Molecular Structure, and Nuclear Magnetic Resonance Study of an Interesting Phosphino-bridged *arachno*-Type Nine-vertex Rhodaborane [2,5-(μ-PPh_2)-1-($PHPh_2$)-2-(η^5-C_5Me_5)-2-RhB_8H_9] *

Xavier L. R. Fontaine, Norman N. Greenwood, John D. Kennedy, Peter MacKinnon, and Mark Thornton-Pett
School of Chemistry, University of Leeds, Leeds LS2 9JT

Reaction of $PHPh_2$ with [6-(η^5-C_5Me_5)-*nido*-6-RhB_9H_{13}] gives an air-stable product [(η^5-C_5Me_5)Rh(μ-PPh_2)B_8H_9($PHPh_2$)] which has been characterized by single-crystal *X*-ray diffraction analysis together with multielement, multiple resonance, and two-dimensional COSY n.m.r. spectroscopy. Crystals (of the 1 : 2 solvate with CH_2Cl_2) are yellow, monoclinic, space group $P2_1/c$, with a = 947.1(2), b = 2 062.2(6), c = 2 208.9(5) pm, β = 91.58(2)°, and Z = 4; final R factor 0.0498 for 4 727 observed reflections. The cluster structure is that of a nine-vertex RhB_8 *arachno* system (*iso*-B_9H_{15} skeletal type) in which the metal atom is on one of the projecting positions on the open face, and in which the PPh_2 group bridges between the metal and a (non-adjacent) projecting boron position on the open face. In spite of this *arachno* formulation, the cluster retains much *nido* nine-vertex character, as judged by geometrical and n.m.r. considerations.

In Part 1 of this series[2] we described the high-yield synthesis of the ten-vertex cluster compound [6-(η^5-C_5Me_5)-*nido*-6-RhB_9H_{13}] [structure (**I**)], and in Part 2[3] its reaction with the tertiary organophosphine PMe_2Ph to give, *inter alia*, the nine-vertex *nido* rhodaborane [2-(η^5-C_5Me_5)-5-(PMe_2Ph)-*nido*-2-RhB_8H_{10}][structure(**II**)]. Here we report that, by contrast, the reaction of [6-(η^5-C_5Me_5)-*nido*-6-RhB_9H_{13}] with the secondary organophosphine $PHPh_2$ yields a compound formulated as [2,5-(μ-PPh_2)-1-($PHPh_2$)-2-(η^5-C_5Me_5)-*arachno*-2-RhB_8H_9] [structure(**III**)] † as its predominant product.

The cluster numbering systems used in this work are given in structures (**IV**) (ten-vertex *nido*) and (**V**) (nine-vertex *nido*).† The numbering in (**V**) differs from those used in recent reports of work on the *nido* nine-vertex skeleton carried out in other laboratories,[4,5] but is the same as our previously used numbering system for work in this area,[3,6-8] and in accord with an IUPAC recommended one.[9]

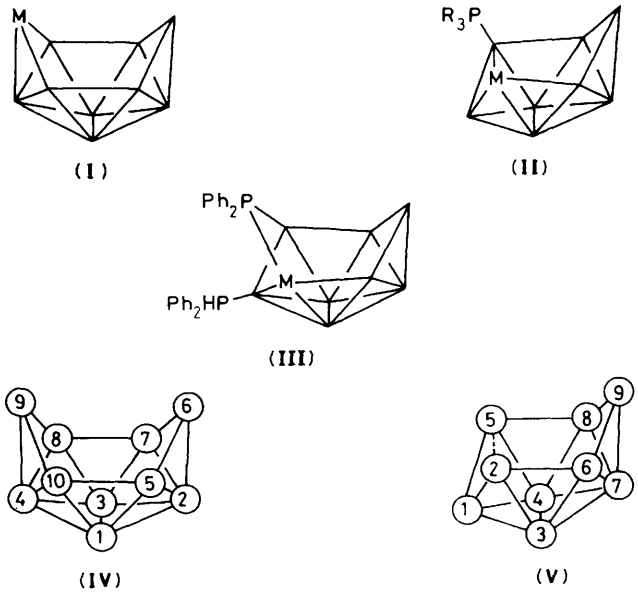

Results and Discussion

The reaction between [6-(η^5-C_5Me_5)-*nido*-6-RhB_9H_{13}] and $PHPh_2$ in dichloromethane solution, followed by heating in toluene solution and chromatographic separation in air, resulted in the formation of [2,5-(μ-PPh_2)-1-($PHPh_2$)-2-(η^5-C_5Me_5)-2-RhB_8H_9] as the predominant metallaborane product. The yellow air-stable crystalline solid was obtained in an isolated yield of 22% and was characterized by single-crystal *X*-ray diffraction analysis. Views of the molecular structure are given in Figure 1, and interatomic distances and angles in Tables 1 and 2 respectively. The phenyl hydrogen atoms were fixed in calculated idealized positions for the crystallographic analysis, whereas the BH and PH hydrogen atoms were located and freely refined.

The compound is seen to be based essentially on the nine-vertex *arachno*-metallanonaborane cluster structure (**VI**) that is well characterized in iridium,[6,10] platinum,[11-14] and gold[15] chemistry, but with, uniquely, a diphenylphosphino moiety bridging from the metal to a non-adjacent boron atom in the open face as depicted in structure (**VII**) [see also (**III**) above]. The metal–phosphorus and boron–phosphorus interatomic distances in this bridge, together with the approximately tetrahedral angles at the phosphorus atom P(2,5), suggest that the bridge is bound to the cluster *via* two two-electron two-centre bonds. There is in addition a $PHPh_2$ phosphine ligand bound *exo* to the cluster at B(1), and two bridging hydrogen atoms are in the (6,9) and (8,9) open-face positions. The Rh(η^5-C_5Me_5) group can be regarded as a straightforward 'octahedral' rhodium(III) centre, which contributes three orbitals to the η^5-

* 1-Diphenylphosphine-2,5-μ-diphenylphosphino-2-(η-pentamethylcyclopentadienyl)-2-rhoda-*nido*-nonaborane.

Supplementary data available: see Instructions for Authors, *J. Chem. Soc., Dalton Trans.*, 1988, Issue 1, pp. xvii—xx.

† Because of the comparisons and parallels with *nido*-type nine-vertex systems (see text) the *nido* nine-vertex numbering system is adopted throughout [structure (**V**)] rather than the *arachno* one. The alternative *arachno* numbering would be [4,8-(μ-PPh_2)-9-($PHPh_2$)-4-(η^5-C_5Me_5)-*iso*-*arachno*-4-RhB_8H_9].

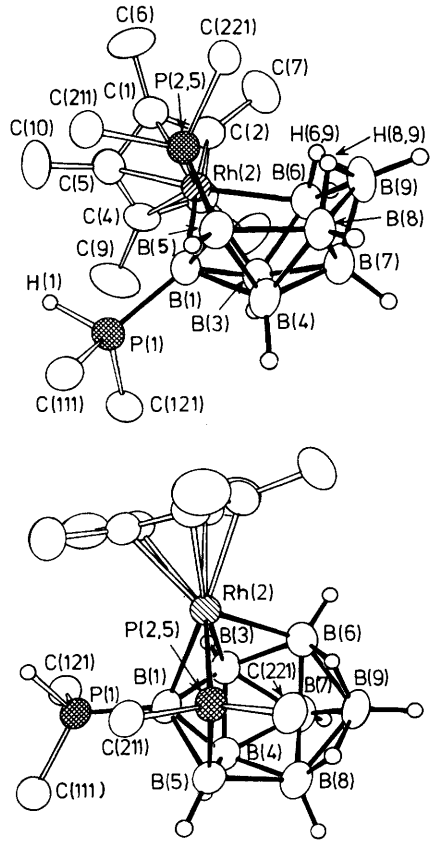

Figure 1. ORTEP drawings of two different views of the crystallographically determined molecular structure of $[(\eta^5\text{-}C_5Me_5)Rh(\mu\text{-}PPh_2)B_8H_9(PHPh_2)]$ with P-phenyl atoms (except for the *ipso* carbon ones) and methyl hydrogen atoms omitted for clarity

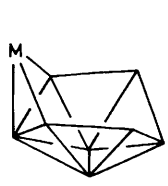

(VI)

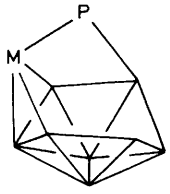

(VII)

C_5Me_5 bonding system, one to the PPh_2 bridge, and two to the cluster bonding proper, so that the metallaborane cluster can then be regarded as an analogue of an *arachno* binary borane $[B_9H_{13}]^{2-}$ of *styx* 2532-type bonding topology.

The structure thus affords an interesting contrast to those of two previously reported nine-vertex metallaboranes, the rhenanonaborane $[2,2,2,2,2\text{-}(PMe_2Ph)_3H_2\text{-}nido\text{-}2\text{-}ReB_8H_{11}]$[8] and the iridaborane $[2,2,2\text{-}(CO)_2(PMe_3)\text{-}nido\text{-}2\text{-}IrB_8H_{11}]$;[6,7] $[2\text{-}(\eta^5\text{-}C_5Me_5)\text{-}5\text{-}(PMe_2Ph)\text{-}nido\text{-}2\text{-}RhB_8H_{10}]$[3] [configuration (**II**)] is also bonded similarly to these two compounds, although it has not been characterized by single-crystal *X*-ray diffraction analysis. Each of these three previously reported species is joined at the M(2)B(5) position *via* a two-electron three-centre M–H–B bridge [*e.g.* Re(2)–B(5) = 252.7 pm[8] and Ir(2)–B(5) = 250.0 pm[7] *versus* 324.1 pm in the rhodium species reported herein], and therefore has *nido* rather than *arachno* nine-vertex character, being closely analogous to *nido*-$[B_9H_{12}]^-$.[8] Notional replacement of the two-electron three-centre M(2)–H–B(5) bridge in the rhenium and iridium compounds by the two two-electron two-centre bonds of the phosphino-bridge in the rhodaborane reported here adds two electrons to the

Table 1. Selected interatomic distances (pm) for $[(\eta^5\text{-}C_5Me_5)Rh(\mu\text{-}PPh_2)B_8H_9(PHPh_2)]$ with estimated standard deviations (e.s.d.s) in parentheses

(*i*) From the rhodium atom

Rh(2)–C(1)	225.3(8)	Rh(2)–B(1)	219.4(9)
Rh(2)–C(2)	225.6(8)	Rh(2)–B(3)	219.2(9)
Rh(2)–C(3)	223.2(8)	Rh(2) ··· B(5)	324.1
Rh(2)–C(4)	226.7(7)	Rh(2)–B(6)	223.1(9)
Rh(2)–C(5)	226.0(8)	Rh(2)–P(2,5)	226.8(3)

(*ii*) Boron–boron

B(1)–B(3)	174.4(11)	B(4)–B(8)	177.7(12)
B(1)–B(4)	171.7(11)	B(5)–B(8)	184.5(11)
B(1)–B(5)	184.0(11)	B(6)–B(7)	177.8(12)
B(3)–B(4)	178.1(11)	B(6)–B(9)	179.8(12)
B(3)–B(6)	179.3(11)	B(7)–B(8)	180.5(12)
B(3)–B(7)	180.0(11)	B(7)–B(9)	168.7(13)
B(4)–B(5)	177.9(11)	B(8)–B(9)	181.2(13)
B(4)–B(7)	177.2(12)		

(*iii*) Boron–hydrogen

B(3)–H(3)	110(5)	B(6)–H(6,9)	121(7)
B(4)–H(4)	123(6)	B(9)–H(6,9)	120(6)
B(5)–H(5)	108(5)	B(9)–H(8,9)	132(5)
B(6)–H(6)	113(5)	B(8)–H(8,9)	122(6)
B(7)–H(7)	121(6)		
B(8)–H(8)	111(5)		
B(9)–H(9)	116(6)		

(*iv*) Other, including selected non-bonding interactions

$C(C_5Me_5)$–$C(C_5Me_5)$	140.3(9)—145.1(9)		
$C(C_5Me_5)$–C(methyl)	151.6(10)—154.8(10)		
B(5)–P(2,5)	190.9(9)	P(2,5)–C(211)	185.5(5)
B(1)–P(1)	191.4(8)	P(2,5)–C(221)	184.8(5)
P(1)–H(1)	142.5(63)	P(1)–Rh(2)	357.0
P(1)–C(111)	180.4(5)	P(2,5)–B(1)	235.0
P(1)–C(121)	179.9(5)	H(1)–Rh(2)	371.5
C(phenyl)–C(phenyl)	139.5*	H(6,9)–Rh(2)	262(7)

* Phenyl groups were refined as rigid regular hexagons with C–C and C–H distances of 139.5 and 108.8 pm respectively.

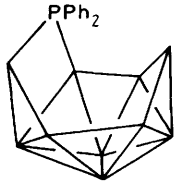

(VIII)

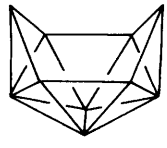

(IX)

formal cluster count and thereby effects a *nido* ⟶ *arachno* transition. This is characterized by an opening of the cluster, as manifested, for example, by open-face angular increases [at B(6) and B(8) of *ca.* 8°, and, more obviously, at B(1) of some 30° as well as the increase in M(2)–B(5) distance mentioned above]. This said, however, the dimensions within the rest of the cluster are very similar for both types of species, for example the 'longer' distance B(5)–B(8) of *ca.* 185 pm appears to be common to both the hydride-bridged and phosphino-bridged compounds, as is the 'shorter' distance B(7)–B(9) of *ca.* 168 pm. The only significant lengthening is perhaps that of B(1)–B(5) [176.4(17) in the rhenium compound to 184.0(11) pm in the rhodaborane], but this is among the atoms in the widening open face. The remainder of the cluster distant from the Rh(2)–P(2,5)–B(5) link therefore retains much *nido* nine-vertex geometrical character (and also electronic character as judged by the n.m.r. studies

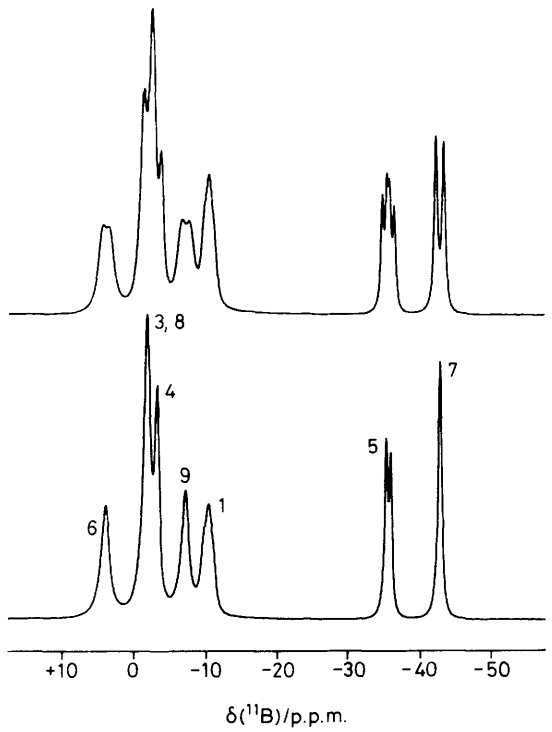

Figure 2. 128-MHz ^{11}B n.m.r. spectra of $[(\eta^5\text{-}C_5Me_5)Rh(\mu\text{-}PPh_2)\text{-}B_8H_9(PHPh_2)]$ in $CD_3C_6D_5$ solution at 363 K. The upper trace is the straightforward ^{11}B spectrum, and the lower trace is the ^{11}B spectrum recorded under conditions of $\{^1H(\text{broad-band noise})\}$ decoupling

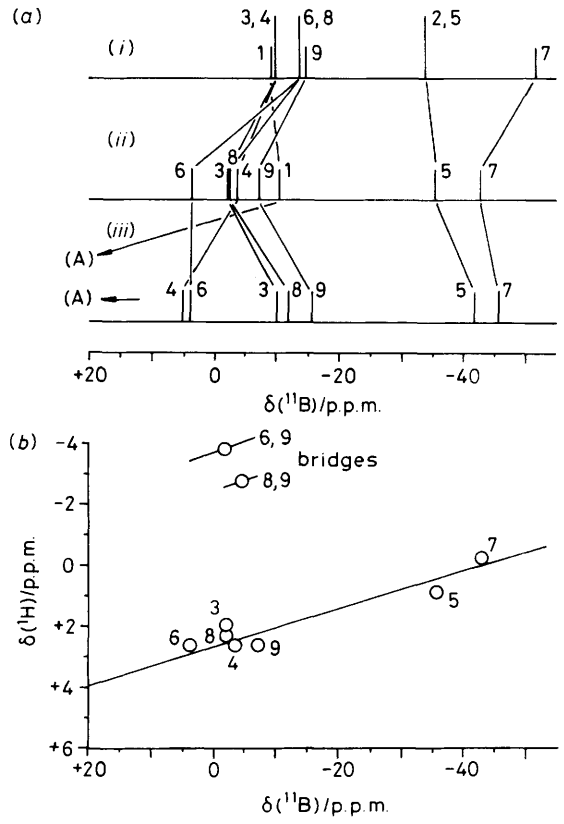

Figure 3. Representations of n.m.r. data for $[(\eta^5\text{-}C_5Me_5)Rh(\mu\text{-}PPh_2)\text{-}B_8H_9(PHPh_2)]$ and related compounds. (*a*) Stick representations of the ^{11}B chemical shifts and relative intensities for $[B_9H_{12}]^-$ (*i*, data from refs. 4, 5, 7, and 8), $[(\eta^5\text{-}C_5Me_5)Rh(\mu\text{-}PPh_2)B_8H_9(PHPh_2)]$ (*ii*, this work), and $[(\eta^5\text{-}C_5Me_5)RhB_8H_{10}(PMe_2Ph)]$ (*iii*, data from ref. 3) respectively. The $^{11}B(1)$ resonance for this last species (A) is off-scale at +39.4 p.p.m. (*b*) Proton–boron-11 shielding correlation plot [same $\delta(^{11}B)$ scale] for hydrogen atoms and their directly-bound boron atoms in $[(\eta^5\text{-}C_5Me_5)Rh(\mu\text{-}PPh_2)B_8H_9(PHPh_2)]$ (CD_2Cl_2 solution). The line drawn has slope $\delta(^{11}B)$:$\delta(^1H)$ of 16:1, intercept $\delta(^1H)$ *ca.* +2.6 p.p.m.

Table 2. Selected angles (°) between interatomic vectors for $[(\eta^5\text{-}C_5Me_5)Rh(\mu\text{-}PPh_2)B_8H_9(PHPh_2)]$, with e.s.d.s in parentheses

(*i*) At the rhodium atom			
B(1)–Rh(2)–B(3)	46.9(2)	P(2,5)–Rh(2)–B(1)	63.6(1)
B(1)–Rh(2)–B(5)	33.0(2)	P(2,5)–Rh(2)–B(3)	95.0(3)
B(1)–Rh(2)–B(6)	85.2(3)	P(2,5)–Rh(2)–B(5)	35.3(1)
B(3)–Rh(2)–B(5)	60.7(2)	P(2,5)–Rh(2)–B(6)	91.9(3)
B(3)–Rh(2)–B(6)	47.8(2)		
B(5)–Rh(2)–B(6)	75.2(2)		
(*ii*) Rhodium boron boron			
Rh(2)–B(1)–B(3)	66.5(4)	Rh(2)–B(3)–B(1)	66.6(4)
Rh(2)–B(1)–B(4)	116.2(5)	Rh(2)–B(3)–B(4)	113.5(5)
Rh(2)–B(1)–B(5)	106.6(5)	Rh(2)–B(3)–B(6)	67.2(4)
		Rh(2)–B(3)–B(7)	118.0(5)
Rh(2)–B(5)–B(1)	40.4(2)	Rh(2)–B(6)–B(3)	64.9(4)
Rh(2)–B(5)–B(4)	77.1(3)	Rh(2)–B(6)–B(7)	117.1(5)
Rh(2)–B(5)–B(8)	94.0(3)	Rh(2)–B(6)–B(9)	124.6(5)
(*iii*) Other angles involving phosphorus			
Rh(2)–P(2,5)–B(5)	101.4(3)	Rh(2)–B(1)–P(1)	120.5(4)
		P(2,5)–B(1)–P(1)	128.3(3)
Rh(2)–P(2,5)–C(211)	114.2(2)	B(3)–B(1)–P(1)	121.5(4)
Rh(2)–P(2,5)–C(221)	120.3(2)	B(4)–B(1)–P(1)	117.3(4)
C(211)–P(2,5)–C(221)	99.1(3)	B(5)–B(1)–P(1)	121.1(4)
(*iv*) Other			
B(1)–B(3)–B(6)	115.8(5)	B(3)–B(6)–B(9)	110.2(5)
B(1)–B(5)–B(8)	106.7(4)	B(5)–B(8)–B(9)	122.0(5)
B(3)–B(1)–B(5)	107.6(4)	B(6)–B(9)–B(8)	102.9(5)
	B–B–H(*exo*)	113(3)—128(3)	
	Rh(2)–B–H(*exo*)	111(3),112(3)	

reported below), the addition of the extra electron pair and concomitant change to *arachno* character being very localized at the Rh(2)B(1)B(7) face. This phenomenon is similar to that observed for 5,6-$(\mu\text{-}PPh_2)\text{-}B_{10}H_{13}$ [structure (**VIII**)] which is notionally derived from *nido*-$B_{10}H_{14}$ [cluster (**IX**)] by the replacement of a two-electron three-centre bridging hydride by the two-electron two-centre bonds of the bridging phosphino link. This compound is formally an *arachno* ten-vertex species but retains much *nido*-decaboranyl character as manifested both structurally and in its n.m.r. properties.[16–18]

The measured n.m.r. parameters for $[(\eta^5\text{-}C_5Me_5)Rh(\mu\text{-}PPh_2)B_8H_9(PHPh_2)]$ are summarized in Table 3, and the ^{11}B n.m.r. spectrum is shown in Figure 2. The n.m.r. properties are entirely consistent with the molecular structure of Figure 1, confirming that the crystal selected was representative of the bulk sample. The eight ^{11}B resonance positions were readily apparent, and selective $^1H\text{-}\{^{11}B\}$ spectroscopy[12,19,20] related the *exo*-terminal ^1H resonance to their directly-bound boron positions and also tentatively assigned the bridging ^1H resonances. The ^{11}B resonances of the two phosphorus-bound boron atoms were readily identified, and sufficient off-diagonal correlations were observable in $[^{11}B\text{–}^{11}B]$-COSY[21] and $[^1H\text{-}^1H]\{^{11}B\}$-COSY[22] experiments thence unambiguously to assign all the ^1H and ^{11}B cluster resonances.

General points to be noted from the n.m.r. results include the

Table 3. Measured n.m.r. data for $[(\eta^5\text{-}C_5Me_5)Rh(\mu\text{-}PPh_2)B_8H_9(PHPh_2)]$[a]

	$CD_3C_6D_5$ solution at 363 K			$CD_3C_6D_5$ solution at 294 K	CD_2Cl_2 solution at 294 K		
Assignment[b]	$\delta(^{11}B)$/p.p.m.[c]	Observed two-dimensional [^{11}B-^{11}B]-COSY correlations[d,e]	$^1J(^{11}B\text{–}^1H)$/Hz[f]	$\delta(^1H)$/p.p.m.[g]	$\delta(^{11}B)$/p.p.m.[c]	$\delta(^1H)$/p.p.m.[g]	Observed two-dimensional [^1H-^1H]-COSY correlations[d,h]
1	−10.6[i]	(3,8w)[j] 4w	*k*	*l*	*ca.* −10.0[o]	+6.48[m]	—
2	Rh	—	—	*l*	Rh	+1.58[n]	—
3	*ca.* −2.0[j]	(1w 4s? 6w 7s)[j]	*ca.* 160[j]	+2.58	*ca.* −3.8[o]	+1.91	7s
4	−3.4	1w (3,8s)[j] 5s 7s	*ca.* 155[j]	+3.41	−5.0	+2.59[p]	(7s 8w 6,9s 8,9s)[p]
5	−35.7[e]	4s	134	+1.63	−37.3[q]	+0.86	8s
6	+3.8	(3,8w)[j] 7w	137[r]	+3.25	+2.8	+2.58[p]	(7s 8w 6,9s 8,9s)[p]
7	−43.0	(3,8w)[j] 4s 6w 9s	144	+1.03	−44.0	−0.22	3s (4,6,9s)[p]
8	*ca.* −2.0[j]	(1w 4s? 6w 7s)[j]	*ca.* 160[j]	+3.39	*ca.* −3.8[o]	+2.29	(4,6,9w)[p] 5s 8,9w
9	−7.3	7s	142[r]	+3.61	*ca.* −10.0[o]	+2.53[p]	(7s 8w 6,9s 8,9s)[p]
6,9 (bridge)	—	—	—	−3.10	—	−3.88[s,t]	(4,6,9s)[p] 8,9w
8,9 (bridge)	—	—	—	−2.20	—	+2.82[t]	(4,6,9s)[p] 8w 6,9w
2,5 (bridge)	P	—	—	—	—	—	—

[a] $\delta(^{31}P)$ −1.01 and −6.97 at 183 K, −1.16 and −6.21 p.p.m. at 253 K; CD_2Cl_2 solution; the more shielded resonance was broad, and the less-shielded exhibited (unresolved) fine structure arising from couplings to ^{103}Rh, ^{31}P, and ^{11}B presumably. [b] Assignments by [^{11}B-^{11}B]- and [^1H-^1H]-COSY correlations (columns 3 and 8), incidence of $^1J(^{31}P\text{–}^{11}B)$, and by selective sharpening of ^1H(bridge) resonances in ^1H-{^{11}B} experiments. [c] ±0.5 p.p.m. to high frequency of BF_3·OEt_2. [d] s = Stronger, w = weaker. [e] Note that strength of observed [^{11}B–^{11}B] correlations will depend on $T_2^*(^{11}B)$ as well as $^1J(^{11}B\text{–}^{11}B)$. [f] ±8 Hz; measured from ^{11}B spectrum with resolution enhancement to achieve maximum separation of doublet components. [g] ±0.05 p.p.m.; $\delta(^1H)$ related to directly-bound ^{11}B positions by ^1H-{^{11}B(selective)} experiments. [h] Measured under conditions of continuous {^{11}B(broad-band noise)} decoupling. [i] Approximate 1:2:1 triplet structure, splitting 86 Hz. [j] Accidental near-coincidence of $^{11}B(3)$ and $^{11}B(8)$ resonances precludes accurate $\delta(^{11}B)$ measurements, the distinguishing of the individual COSY correlations, and accurate $^1J(^{11}B\text{–}^1H)$ measurements; the last also applies to $^{11}B(4)$. [k] P-substituted position. [l] Not measured. [m] PH resonance, $^1J(^{31}P\text{–}^1H)$ 428 Hz; small coupling $J(^{11}B\text{–}^1H)$ revealed by ^1H-{^{11}B} experiments, additional fine structure, splitting ≤1.2 Hz, also probably present. [n] C_5Me_5 resonance, doublet structure arising from $^nJ(^{31}P\text{–}^1H)$ of 1.9 Hz (confirmed by ^1H-{^{31}P} experiments). [o] Accidental near-coincidence of $\delta[^{11}B(1)]$ with $\delta[^{11}B(9)]$, and $\delta[^{11}B(3)]$ with $\delta[^{11}B(8)]$, precludes more accurate $\delta(^{11}B)$ measurements. [p] Accidental near-coincidence of $^1H(4)$, $^1H(6)$, and $^1H(9)$ resonances precludes the distinguishing of the individual COSY correlations. [q] Doublet structure, arising from $^1J(^{31}P\text{–}^{11}B)$ *ca.* 83 Hz in ^{11}B-{^1H(broad-band noise)} spectrum. [r] Not well resolved, $^1J(^{11}B\text{–}^1H)$ may be greater than these observed splittings. [s] Fine structure apparent in ^1H-{^{11}B(broad-band noise)} spectrum. [t] Sufficient selective sharpenings in ^1H-{^{11}B(selective)} experiments to assign these specifically between the μ-6,9 and μ-8,9 positions; it was also found that $|^1J(^{11}B\text{–}^1H)|$ is greater to $^{11}B(9)$ than to $^{11}B(6)$ or $^{11}B(8)$ for these bridging ^1H resonances.

significant absolute and differential changes in $\delta(^{11}B)$ upon change of solvent from CD_2Cl_2 at 294 K to $CD_3C_6D_5$ at 363 K (*cf.* refs. 3, 8, and 23—25), and the general parallel[13,26] between $\delta(^1H)$ of *exo*-terminal hydrogen atoms and $\delta(^{11}B)$ of the cluster boron atoms to which they are bound [see Figure 3(*b*)]. One specific point of interest is the triplet structure for the $^{11}B(1)$ resonance which is retained in the {^{11}B(broad-band noise)} spectrum. This latter must arise from two couplings of similar magnitudes (average *ca.* 85 Hz). One of these will be $^1J[^{31}P(1)\text{–}^{11}B(1)]$, and the second is probably due to $^2J[^{31}P(2,5)\text{–}^{11}B(1)]$; although it could in principle arise instead from $^1J[^{103}Rh(2)\text{–}^{11}B(1)]$. The observed magnitude is anomalously high for either of these two last coupling paths *via endo* cluster linkages,[26] and conversely a value of *ca.* 85 Hz is exceptionally low for $^1J(^{31}P\text{–}^{11}B)$ to an *exo*-terminal phosphine ligand.[26] Comparison data are however limited. A further interesting incidence of ^{31}P coupling is that to the C_5Me_5 protons, presumably arising from a ^4J path to P(2,5) although a ^5J pathway to P(1) cannot be excluded on present evidence (*cf.* ^5J or ^6J pathways in Table 6 of Part 2).[3]

One striking aspect of the assigned cluster ^{11}B and ^1H n.m.r. spectra is the remarkable similarity to those[4,5,8] of the *nido* nine-vertex anion $[B_9H_{12}]^-$ [see Figure 3 (*a*)(*i*) and (*ii*)]. Although the rhodaborane is now of a more open *arachno* configuration, and also has a phosphino bridge, an *exo*-terminal phosphine ligand, and one of the open-face BH vertices subrogated by $Rh(\eta^5\text{-}C_5Me_5)$, the basic cluster shielding pattern is retained. This suggests a gross electronic similarity with the *nido* nine-vertex cluster, reinforcing the same conclusion drawn from the geometrical considerations discussed above. However, it must be pointed out that the $^{11}B(1)$ resonance of the previously reported[3] compound $[(\eta^5\text{-}C_5Me_5)RhB_8H_{10}(PMe_2Ph)]$, which has a more straightforward *nido* nine-vertex geometry and is therefore expected to parallel the behaviour of $[B_9H_{12}]^-$ even more closely, exhibits a large shift of some 50 p.p.m. to lower field [Figure 3(*a*) (*iii*)].[8] Apart from this, though, the cluster shielding pattern again conforms reasonably closely to that of *nido*-$[B_9H_{12}]^-$.

Experimental

Preparation of $[(\eta^5\text{-}C_5Me_5)Rh(\mu\text{-}PPh_2)B_8H_9(PHPh_2)]$.—$[6\text{-}(\eta^5\text{-}C_5Me_5)\text{-}nido\text{-}6\text{-}RhB_9H_{13}]$ (0.305 g, 0.875 mmol; prepared as described in Part 1[2]) was dissolved in dry, degassed CH_2Cl_2 (30 cm^3). $PHPh_2$ (0.345 g, 1.85 mmol), prepared from the reaction of PPh_2Cl with $LiAlH_4$,[27] was added by syringe, and the solution stirred at room temperature under nitrogen. During the following 3 d consumption of the starting rhodaborane complex was monitored (analytical t.l.c.) and showed that little or no reaction had occurred. The solvent was removed and replaced with dry, degassed toluene (30 cm^3) and the reaction mixture heated at reflux for 1 h yielding a brown-red solution. The mixture was cooled, evaporated to dryness, and the residue dissolved in CH_2Cl_2 (*ca.* 5 cm^3) and applied to a series of preparative t.l.c. plates (Kieselgel GF 254, Fluka, plates 200 × 200 × 1 mm). Elution with CH_2Cl_2–hexane (75:25) gave a yellow component with R_f = 0.61. Further purification by repeated chromatography using CH_2Cl_2–hexane (50:50) as eluant (R_f now 0.41) gave pure $[(\eta^5\text{-}C_5Me_5)Rh(\mu\text{-}PPh_2)B_8H_9(PHPh_2)]$ and crystallization from CH_2Cl_2–hexane gave the 1:2 CH_2Cl_2 solvate (0.166 g, 0.190 mmol, 21.7%) (Found: C, 49.8; H, 5.75; B, 10.0. $C_{36}H_{49}B_8Cl_4P_2Rh$ requires C,

Table 4. Atomic co-ordinates ($\times 10^4$) for [2,5-(μ-PPh_2)-1-($PHPh_2$)-2-(η^5-C_5Me_5)-2-RhB_8H_9]

Atom	*x*	*y*	*z*	Atom	*x*	*y*	*z*
Rh(2)	2 894.7(4)	2 381.8(2)	2 305.1(2)	B(6)	638(7)	2 554(4)	2 521(3)
P(1)	4 990(2)	2 698(1)	3 641(1)	B(7)	218(7)	2 597(4)	3 299(4)
P(2,5)	2 882(2)	1 395(1)	2 758(1)	B(8)	533(7)	1 784(4)	3 575(4)
C(111)	5 683(4)	2 300(2)	4 313(1)	B(9)	−475(7)	1 978(4)	2 889(4)
C(112)	7 127(4)	2 169(2)	4 361(1)	Cl(1)	7 900(4)	3 711(2)	5 434(2)
C(113)	7 695(4)	1 884(2)	4 886(1)	Cl(2)	10 420(5)	4 093(2)	4 903(2)
C(114)	6 819(4)	1 729(2)	5 363(1)	Cl(3a)	4 903(17)	4 864(5)	582(5)
C(115)	5 376(4)	1 860(2)	5 315(1)	Cl(3b)	9 745(14)	4 759(7)	612(6)
C(116)	4 808(4)	2 146(2)	4 790(1)	C(1b)	9 061(12)	3 572(6)	4 841(5)
C(121)	5 041(4)	3 547(1)	3 826(2)	C(25a)	5 635(42)	5 164(20)	250(19)
C(122)	3 906(4)	3 826(1)	4 120(2)	C(25b)	10 867(43)	4 355(20)	111(19)
C(123)	3 978(4)	4 470(1)	4 309(2)	H(112)	7 805(4)	2 289(2)	3 992(1)
C(124)	5 185(4)	4 837(1)	4 204(2)	H(113)	8 813(4)	1 782(2)	4 924(1)
C(125)	6 320(4)	4 558(1)	3 910(2)	H(114)	7 259(4)	1 508(2)	5 769(1)
C(126)	6 247(4)	3 913(1)	3 720(2)	H(115)	4 698(4)	1 741(2)	5 684(1)
C(211)	4 620(3)	987(2)	2 791(2)	H(116)	3 690(4)	2 247(2)	4 753(1)
C(212)	5 522(3)	1 065(2)	3 295(2)	H(122)	2 971(4)	3 542(1)	4 202(2)
C(213)	6 870(3)	792(2)	3 300(2)	H(123)	3 100(4)	4 686(1)	4 537(2)
C(214)	7 316(3)	441(2)	2 800(2)	H(124)	5 241(4)	5 336(1)	4 351(2)
C(215)	6 413(3)	363(2)	2 296(2)	H(125)	7 254(4)	4 842(1)	3 828(2)
C(216)	5 065(3)	636(2)	2 291(2)	H(126)	7 126(4)	3 698(1)	3 493(2)
C(221)	1 801(4)	725(2)	2 429(2)	H(212)	5 178(3)	1 337(2)	3 682(2)
C(222)	1 820(4)	130(2)	2 729(2)	H(213)	7 569(3)	853(2)	3 691(2)
C(223)	1 056(4)	−393(2)	2 490(2)	H(214)	8 359(3)	230(2)	2 804(2)
C(224)	273(4)	−321(2)	1 949(2)	H(215)	6 758(3)	91(2)	1 909(2)
C(225)	255(4)	275(2)	1 649(2)	H(216)	4 366(3)	575(2)	1 901(2)
C(226)	1 019(4)	798(2)	1 889(2)	H(222)	2 426(4)	74(2)	3 147(2)
C(1)	3 695(6)	2 198(3)	1 369(3)	H(223)	1 070(4)	−853(2)	2 722(2)
C(2)	2 548(7)	2 640(3)	1 320(3)	H(224)	−318(4)	−725(2)	1 764(2)
C(3)	2 938(6)	3 206(3)	1 651(3)	H(225)	−351(4)	331(2)	1 231(2)
C(4)	4 330(7)	3 129(3)	1 888(2)	H(226)	1 004(4)	1 258(2)	1 656(2)
C(5)	4 808(6)	2 510(3)	1 728(3)	H(3)	2 119(51)	3 414(27)	3 040(22)
C(6)	3 868(9)	1 576(3)	1 012(3)	H(4)	1 872(61)	2 589(25)	4 252(27)
C(7)	1 228(8)	2 558(4)	920(3)	H(5)	2 865(54)	1 343(26)	3 949(24)
C(8)	2 054(9)	3 836(3)	1 672(3)	H(6)	65(54)	2 847(25)	2 156(24)
C(9)	5 198(9)	3 671(4)	2 197(3)	H(7)	−640(64)	2 968(30)	3 498(26)
C(10)	6 297(7)	2 236(4)	1 831(3)	H(8)	39(51)	1 543(23)	3 942(22)
B(1)	3 261(7)	2 371(3)	3 290(3)	H(9)	−1 676(63)	1 906(27)	2 788(25)
B(3)	1 900(7)	2 889(3)	3 054(3)	H(6,9)	294(68)	1 994(32)	2 465(29)
B(4)	1 784(7)	2 411(3)	3 722(3)	H(8,9)	164(53)	1 468(26)	3 132(24)
B(5)	2 448(7)	1 622(3)	3 570(3)	H(1P)	6 155(65)	2 616(28)	3 253(28)

Table 5. Experimental details for two-dimensional n.m.r. experiments

Experiment	[^{11}B–^{11}B]-COSY	[^{1}H–^{1}H]-COSY
Data size (t_2,t_1)/words	256,64	512,128
Transform size (F_2,F_1)/words	256,128	512,256
t_2 Sweep width (= 2 × t_1 sweep width)/Hz	7 575.8	5 618.0
Digital resolution (F_2,F_1)/Hz per point	59.2	21·9
No. of transients per t_1 increment	512	400
Recycling time/s	0.070	1.05
Mixing pulse/°	45	45
Window*(t_2 and t_1)	sine-bell	sine-bell squared
Temperature/K	363	294

* Centred on centre of free induction decay prior to zero-filling to transform size.

49.4; H, 5.65; B, 9.9%). Mass spectrum: base peak in highest mass envelope at *m/e* 708 [$M^+ - 2CH_2Cl_2$]; calculated for $^{12}C_{34}{}^1H_{45}{}^{11}B_8{}^{31}P_2{}^{103}Rh$, 706. Single crystals suitable for an *X*-ray diffraction analysis were grown by layering a CH_2Cl_2 solution of the compound with hexane and were sealed in epoxy resin to prevent loss of solvent of crystallization.

X-Ray Crystallography.—Crystals suitable for *X*-ray structural analysis were grown by the diffusion of hexane into a dichloromethane solution of the title compound as described above. All measurements were made on a Nicolet P3/F diffractometer operating in the ω–2θ scan mode using graphite monochromated Mo-K_α radiation (λ = 71.069 pm) following a procedure described in detail elsewhere.[28] The data set was corrected for absorption once the structure had been solved.[29]

Crystal data. $C_{36}H_{49}B_8Cl_4P_2Rh$, M = 874.88, monoclinic, a = 947.1(2), b = 2 062.2(6), c = 2 208.9(5) pm, β = 91.58(2)°, U = 4.313 nm^3, space group $P2_1/c$, Z = 4, D_c = 1.347 g cm^{-3}, μ(Mo-K_α) = 6.67 cm^{-1}, F(000) = 1 500.

Data collection parameters. Scans running from 1° below K_{α_1} to 1° above K_{α_2}, scan speeds 2.0—29.2° min^{-1}, 4.0 ⩽ 2θ ⩽ 45.0°. 6 003 Data were collected, 4 727 being considered observed [$I > 2.0\sigma(I)$].

Refinement. Number of variables = 499, weighting factor g = 0.0004, final R and R' 0.0498 and 0.0524 respectively.

The structure was determined *via* standard heavy-atom techniques and refined by full-matrix least squares using SHELX 76.[30] All non-hydrogen atoms other than the carbon atoms of both solvent molecules (one of which was found to be disordered around a symmetry centre) were assigned anisotropic thermal parameters, with the phenyl groups treated as rigid bodies and refined with idealized hexagonal symmetry (C–H = 139.5 pm). The disordered CH_2Cl_2 molecule was treated in terms of partially occupied chlorine and carbon atom

sites for which the occupancies summed to 1.0 and 0.5 respectively. (These atoms were all assigned individual isotropic thermal parameters.) All phenyl and methyl hydrogen atoms were included in calculated positions (C–H = 108 pm) and assigned to an overall isotropic thermal parameter for each ligand. The weighting scheme $w = [\sigma^2(F_o) + g(F_o)^2]^{-1}$ was used in which the parameter g was included in refinement in order to obtain a flat analysis of variance with increasing sin θ and $(F/F_{max.})^{\frac{1}{2}}$. Fractional atomic co-ordinates are given in Table 4.

Additional material available from the Cambridge Crystallographic Data Centre comprises thermal parameters and remaining bond distances and angles.

Nuclear Magnetic Resonance Spectroscopy.—This was performed at 2.35 and 9.40 Tesla on commercially available instrumentation. The techniques of ^1H-$\{^{11}B\}$ spectroscopy,[12,19,20,31] $[^{11}B$–$^{11}B]$-COSY spectroscopy,[1–3,8,32,33] and $[^1H$–$^1H]$-COSY spectroscopy[1,8,22,32] as applied to this work were essentially as described elsewhere, particular details for the COSY work being summarized in Table 5. In the $[^{11}B$–$^{11}B]$ COSY work a high temperature was used in order to minimise ^{11}B relaxation rates,[22] and in the ^1H-$\{^{11}B\}$ work use was made of the technique in which a ^1H-$\{^{11}B$(off-resonance)$\}$ spectrum is subtracted from a ^1H-$\{^{11}B$(on-resonance)$\}$ spectrum in order to remove lines not coupled to the ^{11}B nucleus in question.[12,34] Other n.m.r. spectroscopy was straightforward. Chemical shifts $\delta(^1H)$, $\delta(^{31}P)$, and $\delta(^{11}B)$ are given in p.p.m. to high frequency (low field) of Ξ 100 (internal $SiMe_4$), Ξ 40.480 730 (nominally 85% H_3PO_4), and Ξ 32.083 971 MHz (nominally $BF_3{\cdot}OEt_2$ in $CDCl_3$)[26] respectively (Ξ being defined as in ref. 35).

Acknowledgements

We thank the S.E.R.C. for support and the University of Leeds Research Fund for an equipment grant (to M. T-P. and J. D. K.)

References

1 Part 3, X. L. R. Fontaine, H. Fowkes, N. N. Greenwood, J. D. Kennedy, and M. Thornton-Pett, *J. Chem. Soc., Dalton Trans.*, 1987, 2417.
2 X. L. R. Fontaine, H. Fowkes, N. N. Greenwood, J. D. Kennedy, and M. Thornton-Pett, *J. Chem. Soc., Dalton Trans.*, 1986, 547.
3 X. L. R. Fontaine, H. Fowkes, N. N. Greenwood, J. D. Kennedy, and M. Thornton-Pett, *J. Chem. Soc., Dalton Trans.*, 1987, 1431.
4 G. B. Jacobsen, D. G. Meina, J. H. Morris, C. Thompson, S. J. Andrews, D. Reed, A. J. Welch, and D. F. Gaines, *J. Chem. Soc., Dalton Trans.*, 1985, 1645.
5 S. Heřmánek, J. Fusek, B. Štíbr, J. Plešek, and T. Jelínek, *Polyhedron*, 1986, **5**, 1873.
6 J. Bould, J. E. Crook, N. N. Greenwood, J. D. Kennedy, and W. S. McDonald, *J. Chem. Soc., Chem. Commun.*, 1982, 346.
7 J. Bould, N. N. Greenwood, and J. D. Kennedy, *J. Chem. Soc., Dalton Trans.*, 1984, 2477.
8 M. A. Beckett, M. Bown, X. L. R. Fontaine, N. N. Greenwood, J. D. Kennedy, and M. Thornton-Pett, *J. Chem. Soc., Dalton Trans.*, 1988, 1969.
9 IUPAC Commission on Nomenclature of Inorganic Chemistry, *Pure Appl. Chem.*, 1972, **30**, 683.
10 J. Bould, J. E. Crook, N. N. Greenwood, and J. D. Kennedy, *J. Chem. Soc., Dalton Trans.*, 1984, 1903.
11 A. R. Kane, L. J. Guggenberger, and E. L. Muetterties, *J. Am. Chem. Soc.*, 1970, **92**, 2571.
12 S. K. Boocock, N. N. Greenwood, M. J. Hails, J. D. Kennedy, and W. S. McDonald, *J. Chem. Soc., Dalton Trans.*, 1981, 1415.
13 N. N. Greenwood, M. J. Hails, J. D. Kennedy, and W. S. McDonald, *J. Chem. Soc., Dalton Trans.*, 1985, 953.
14 R. Ahmad, J. E. Crook, N. N. Greenwood, and J. D. Kennedy, *J. Chem. Soc., Dalton Trans.*, 1986, 2433.
15 M. A. Beckett, J. E. Crook, N. N. Greenwood, and J. D. Kennedy, *J. Chem. Soc., Dalton Trans.*, 1984, 1427.
16 L. B. Friedman and S. L. Perry, *Inorg. Chem.*, 1973, **12**, 288.
17 M. A. Beckett and J. D. Kennedy, *J. Chem. Soc., Chem. Commun.*, 1983, 575.
18 M. Thornton-Pett, M. A. Beckett, and J. D. Kennedy, *J. Chem. Soc., Dalton Trans.*, 1986, 303.
19 J. D. Kennedy and N. N. Greenwood, *Inorg. Chim. Acta*, 1980, **38**, 33.
20 J. D. Kennedy and B. Wrackmeyer, *J. Magn. Reson.*, 1980, **38**, 529.
21 T. L. Venable, W. C. Hutton, and R. N. Grimes, *J. Am. Chem. Soc.*, 1984, **106**, 29.
22 X. L. R. Fontaine and J. D. Kennedy, *J. Chem. Soc., Chem. Commun.*, 1986, 779.
23 M. A. Beckett, J. E. Crook, N. N. Greenwood, and J. D. Kennedy, *J. Chem. Soc., Dalton Trans.*, 1986, 1879.
24 T. L. Venable, C. T. Brewer, and R. N. Grimes, *Inorg. Chem.*, 1985, **24**, 4751.
25 D. F. Gaines, C. K. Nelson, J. C. Kunz, J. H. Morris, and D. Reed, *Inorg. Chem.*, 1984, **23**, 3252.
26 J. D. Kennedy, in 'Multinuclear N.M.R.,' ed. J. Mason, Plenum, London and New York, 1987, ch. 8, pp. 221—254 and refs. therein.
27 W. E. Hatfield and J. T. Yoke, *Inorg. Chem.*, 1962, **1**, 470.
28 A. Modinos and P. Woodward, *J. Chem. Soc., Dalton Trans.*, 1974, 2065.
29 N. Walker and D. Stuart, *Acta Crystallogr., Sect. A*, 1983, **39**, 158.
30 G. M. Sheldrick, SHELX 76, Program System for *X*-Ray Structure Determination, University of Cambridge, 1976.
31 X. L. R. Fontaine and J. D. Kennedy, *J. Chem. Soc., Dalton Trans.*, 1987, 1513.
32 M. Bown, X. L. R. Fontaine, N. N. Greenwood, and J. D. Kennedy, *J. Organomet. Chem.*, 1984, **325**, 233.
33 M. Bown, X. L. R. Fontaine, N. N. Greenwood, J. D. Kennedy, and M. Thornton-Pett, *J. Chem. Soc., Dalton Trans.*, 1987, 1169.
34 J. D. Kennedy and J. Staves, *Z. Naturforsch., Teil B*, 1979, **34**, 808.
35 W. McFarlane, *Proc. R. Soc. London, Ser. A*, 1968, **306**, 185.

Received 14*th August* 1987; *Paper* 7/1502